OPTIMIZATION OF PROPELLERS USING HELICOIDAL VORTEX MODEL

Article · January 2003

DOI: 10.1142/9789812796837_0022

1 author:

J.J. Chattot
University of California, Davis
125 PUBLICATIONS **796** CITATIONS

OPTIMIZATION OF PROPELLERS USING HELICOIDAL VORTEX MODEL

Jean-Jacques CHATTOT †

Abstract

An approach to the optimization of propellers is presented that is based on a helicoidal vortex model and the rigorous calculation of the induced velocities to maximize the thrust for a given output torque of the engine. The mathematical model is presented and the discretized equations are derived for the inviscid model and for the viscous correction. The design of a two-bladed propeller at low advance ratio is carried out and the distributions of circulation, induced velocities, chord and twist are obtained. Comparison with published data indicates that the method is efficient and flexible and produces detailed and accurate results.

Key Words:

1 Introduction

The aerodynamics of propellers, rotors and more generally of rotating machinery is a challenging topic, even today, despite the advances in computing power. This is due to the many flow features and scales that need to be accounted for. Among these, flow unsteadiness remains one of the pacing items in the simulation of blade/wake interaction in a turbomachinery or of a helicopter rotor in advance flight. In simpler situations steady flow can be considered a reasonable model, as in the case of a helicopter in hover or a propeller moving parallel to its axis, yet the intrinsic difficulty of such flows remains in the prediction and calculation of the vortex structure created downstream of the blades. The inviscid model has been described in landmark papers and books by Prandtl and Betz [1], Glauert [2], Goldstein [3], Lock [4] and Theodorsen [5]. For large Reynolds numbers the model is expected to remain accurate and give a correct representation of the blade/vortex sheet interaction, even though the flow contraction behind the blades is generally neglected. This helicoidal structure is the most important aspect of propeller flow as it influences the blade operation through the induced velocities in the streamline and azimuthal direction, which in turn determine the local angle of attack of the blade element, its lift and induced drag.

Received on.

† University of California Davis, Davis, CA 95616

The vortex sheet is a free surface and its location and strength are part of the solution. However, capturing the vortex sheet beyond 2 or 3 turns of the helix with an Euler or Navier-Stokes solver is beyond the current capabilities of modern computational fluid dynamics (CFD), rendering the simulation inaccurate for analysis or design purposes. The present work is based on the Goldstein model with a helicoidal vortex structure depending on the advance ratio $adv = \dfrac{V}{\Omega R}$, the power coefficient $P_\tau = \dfrac{2P}{\rho\Omega^3 R^5}$ and the root location y_0. This is an improvement on the method of Adkins and Liebeck [6] who combine the actuator disk and rotor blade element equations, the so-called the blade element theory (or vortex theory, see [7]). In the latter approach, the flows in elementary stream tubes behind the propeller are independent of one another. This is an approximation inherent to this model and it is believed to be acceptable for a large number of blades and low advance ratios. In reality, the helicoidal nature of the sheet always allows interaction to take place between the blade sections, in a way similar to the flow on a wing.

Once the vortex structure is defined, the Biot-Savart law is used to obtain the influence coefficients relating the vortex strength $\dfrac{d\Gamma}{dy}$ to the induced axial and azimuthal (downwash) velocities $u(y)$ and $w(y)$. The induced axial velocity $u(y)$ is due to the winding of the sheet behind the rotor and goes to zero for a single wing in translation or for a very large advance ratio. The Goldstein model combined with the Biot-Savart law removes some of the empirism as-

sociated with the actuator disk/annulus flow model. There remains, however, the assumption of a frozen vortex structure; more details are given in the next section. In reference [3], Goldstein finds a particular analytic solution for the flow past a regular screw surface starting from the root at $y_0 = 0$. Here we make use of the computer resources available today to evaluate the influence coefficients of the vortex sheet on the blade and to use a minimization procedure to find the solution $\Gamma(y)$ as well as the geometry of the optimum blade. Optimization proceeds along the line of a previous paper [8]. A viscous correction is added to the model using strip theory and two-dimensional viscous profile data. This is assumed to be acceptable since the objective is to design a large Reynolds number propeller with best possible performance and a realistic lift coefficient distribution. This does not presume how the propeller will perform in off-design conditions.

2 Helicoidal vortex structure

The minimum energy loss condition of Betz [1] requires the vortex sheet to be a regular screw surface. The pitch of the screw varies with the average axial velocity, as estimated by the actuator disk momentum theorem, from u_b at the blade plane to $u_T = 2u_b$ in the Trefftz plane, far downstream. This flow acceleration is accompanied by a contraction of the stream tube which will be neglected. The theory predicts that the thrust of the propeller is

$T = -2\pi\rho R^2(V + u_b)u_b$

and the power delivered by the propeller

$P = 2\pi\rho R^2(V + u_b)^2 u_b$

Dimensionless quantities are introduced such as the thrust coefficient acting opposite to the drag (negative drag)

$$C_D = -\frac{2T}{\rho V^2 R^2}$$

the lift coefficient (in the case of a wing)

$$C_L = \frac{2L}{\rho V^2 R^2}$$

the torque coefficient

$$C_\tau = \frac{2\tau}{\rho V^2 R^3} = \frac{P_\tau}{adv^2}$$

the power coefficient P_τ , given above, and all the coordinates, velocities, circulation and chord distribution as

$x = R\widetilde{x}$

$y = R\widetilde{y}$

$z = R\widetilde{z}$

$u = V\widetilde{u}$

$v = V\widetilde{v}$

$w = V\widetilde{w}$

$\Gamma = VR\widetilde{\Gamma}$

$c = R\widetilde{c}$

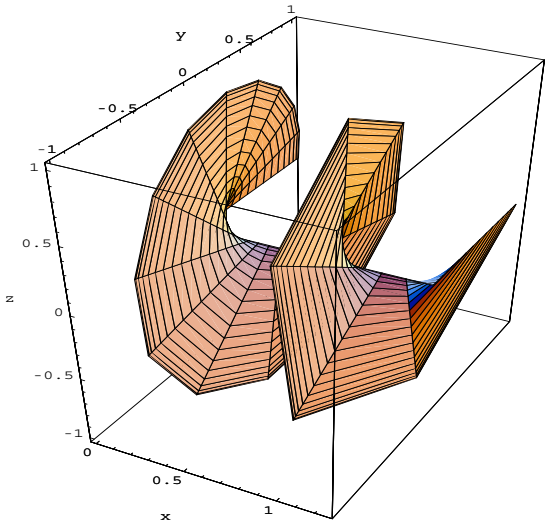

Fig.1: Partial view of the vortex sheet behind a propeller blade

Unless otherwise indicated, the dimensionless variables are used in the rest of the paper and the tilde is dropped for simplicity. The induced velocities on the blade are given by the Biot-Savart law

$$u(y') = \int_{y_0}^{1}\int_{0}^{\infty} \frac{1}{4\pi}\frac{d\Gamma(y)}{dy}\frac{(y'-y_v)\dfrac{dz_v}{dx} + z_v\dfrac{dy_v}{dx}}{\left[x^2+(y'-y_v)^2+z_v^2\right]^{3/2}}dxdy \quad (1)$$

$$w(y') = -\int_{y_0}^{1}\int_{0}^{\infty} \frac{1}{4\pi}\frac{d\Gamma(y)}{dy}\frac{(y'-y_v) + x\dfrac{dy_v}{dx}}{\left[x^2+(y'-y_v)^2+z_v^2\right]^{3/2}}dxdy \quad (2)$$

where the equation of the vortex sheet is given by

$$\begin{cases} y_v = y\cos\left(\dfrac{x}{adv}\right) \\ z_v = y\sin\left(\dfrac{x}{adv}\right) \end{cases} \quad x \geq 0,\ y_0 \leq y \leq 1 \quad (3)$$

A vortex filament corresponds to a fixed value of y. Two turns of the vortex sheet shed by one blade is shown in figure 1. Note that the influence of the other blades must be accounted for, which can be done in the case of a two-bladed propeller by changing y' in $-y'$ and using symmetry arguments.

It can be seen that the induced velocities are even functions of x, hence, in the Trefftz plane, where the integration runs from $-\infty$ to $+\infty$, the contributions are doubled in agreement with the momentum theorem.

The increase in induced axial velocity from u_b to u_T is reflected in the stretching in the construction of the helix. This is accomplished with a variable adv in the above equations, that increases from $adv(1+u_b)$ to $adv(1+2u_b)$ on three turns of the screw. Numerical tests have shown that little difference in results occur when the stretching is done on one or five turns.

In general, the power delivered to the propeller is known. It is a function of the rotation speed Ω. In the application, the power will be assumed constant for simplicity. The average axial velocity u_b can be computed using the above formula for P. The value u_b and the advance ratio parameter adv are the two major parameters defining the vortex structure.

The discrete vortex sheet is constructed as a vortex lattice. In the x-direction, a variable step allows for the clustering of points near the blade where the integrand in the Biot-Savart formulae is large. However the stretching is limited to a point where there remains at least 4 points on a turn, until a sufficient distance L from the rotor is reached, typically 20 radii. Beyond this position, an asymptotic formula is used. In the y-direction, a cosine distribution of control points is used as is done for the lifting line problem:

$$x_i = x_{i-1} + dx_i \ , \ dx_i = s dx_{i-1} \ , \ i = 1, ..., ix \quad y'_j = y_0 + (1-y_0)\cos\theta_j \ , \ \theta_j = \frac{j-1}{jx-1}\pi \ , \ j = 1, ..., jx$$

with the following choice of parameters $x_0 = 0$, $dx_0 = 1.0\,10^{-6}$, $s = 1.001$, $ix = 10, 001$, $jx = 101$

Integration points are placed between the control points to avoid the singularity in the integrand as in [8]: $y_k = y_0 + (1-y_0)\cos(\theta_k + \dfrac{\Delta\theta}{2})$, $\Delta\theta = \dfrac{\pi}{jx-1}$, $k = 1, ..., jx-1$

The induced velocities are given by

$$w_k = \sum_{j=1}^{jx-1} (\Gamma_{j+1} - \Gamma_j) a_{j,k} \qquad u_k = \sum_{j=1}^{jx-1} (\Gamma_{j+1} - \Gamma_j) b_{j,k}$$

where

$$a_{j,k} = -\sum_{i=2}^{ix} \frac{1}{4\pi} \frac{\left(y'_k - \left(\dfrac{y_{v\,i-1} + y_{v\,i}}{2} \right)_j \right)(x_i - x_{i-1}) + \left(\dfrac{x_{i-1} + x_i}{2} \right)(y_{v\,i} - y_{v\,i-1})_j}{\left[\left(\dfrac{x_{i-1} + x_i}{2} \right)_j^2 + \left(y'_k - \left(\dfrac{y_{v\,i-1} + y_{v\,i}}{2} \right)_j \right)^2 + \left(\dfrac{z_{v\,i-1} + z_{v\,i}}{2} \right)_j^2 \right]^{\frac{3}{2}}} \tag{4}$$

$$b_{j,k} = \sum_{i=2}^{ix} \frac{1}{4\pi} \frac{\left(y'_k - \left(\dfrac{y_{v\,i-1} + y_{v\,i}}{2} \right)_j \right)(z_{\,vi} - z_{v\,i-1})_j + \left(\dfrac{z_{v\,i-1} + z_{v\,i}}{2} \right)_j (y_{v\,i} - y_{v\,i-1})_j}{\left[\left(\dfrac{x_{i-1} + x_i}{2} \right)_j^2 + \left(y'_k - \left(\dfrac{y_{v\,i-1} + y_{v\,i}}{2} \right)_j \right)^2 + \left(\dfrac{z_{v\,i-1} + z_{v\,i}}{2} \right)_j^2 \right]^{\frac{3}{2}}} \tag{5}$$

The asymptotic remainders are found to be

$$\Delta a_{j,k} = \frac{1}{4\pi} \frac{y'_k - 2y_j \cos\left(\dfrac{L}{adv}\right)}{2L^2} + O\left(\frac{adv}{L^3}\right) \qquad \Delta b_{j,k} = -\frac{1}{4\pi} \frac{y_j^2}{advL^2} + O\left(\frac{1}{L^3}\right) \tag{6}$$

3 Inviscid model

Having constructed the vortex sheet, as detailed in the previous section, the strip theory is used to relate locally the circulation to the thrust and the torque. In dimensional form, for an element dy of blade in inviscid flow, according to the Kutta-Joukowski Lift theorem, the force $d\overrightarrow{F}(y)$ is acting perpendicular to the local incoming flow $\overrightarrow{q}(y)$ and equals $d\overrightarrow{F}(y) = \rho\,\overrightarrow{q}(y) \wedge \Gamma(y)\,\overrightarrow{j}\,dy$.

In dimensionless form, the elementary contributions to drag (negative), lift and torque coefficients are respectively

$$dC_D = -2\Gamma(y)\left(\frac{y}{adv} + w(y)\right)dy \qquad dC_L = 2\Gamma(y)\,(1+u(y))\,dy \qquad dC_\tau = 2\Gamma(y)\,(1+u(y))\,y dy \tag{7}$$

For a two bladed rotor, the resulting force and moment coefficients are

$$C_D = -4\int_{y_0}^{1}\Gamma(y)\left(\frac{y}{adv} + w(y)\right)dy \quad C_L = 4\int_{y_0}^{1}\Gamma(y)\,(1+u(y))\,dy \quad C_\tau = 4\int_{y_0}^{1}\Gamma(y)\,(1+u(y))\,y dy \tag{8}$$

Note that for an infinite advance ratio and $y_0 = -1$ the above formulae reduce to the lifting line results for a wing.

Discrete analogs are now defined:

$$\begin{cases} C_D = -4\displaystyle\sum_{k=2}^{jx-1}\Gamma_k\left(\frac{y'_k}{adv} + w_k\right)(y_k - y_{k-1}) \\ C_L = 4\displaystyle\sum_{k=2}^{jx-1}\Gamma_k\,(1+u_k)\,(y_k - y_{k-1}) \\ C_\tau = 4\displaystyle\sum_{k=2}^{jx-1}\Gamma_k\,(1+u_k)\,y'_k(y_k - y_{k-1}) \end{cases} \tag{9}$$

Minimization of the induced drag amounts to maximizing the thrust. Taking derivatives with respect to the discrete values Γ_j results in the following equations:

$$\frac{\partial C_D}{\partial \Gamma_j} = -4\left(\frac{y'_j}{adv} + w_j\right)(y_j - y_{j-1}) - 4\sum_{k=2}^{jx-1}\Gamma_k(a_{j-1,k} - a_{j,k})(y_k - y_{k-1}) = 0\ , \quad j = 2, \cdots, jx-1 \tag{10}$$

$$\Gamma_1 = \Gamma_{jx} = 0 \tag{11}$$

This is a linear non-homogeneous system for the Γ_j's where the rotation term $\dfrac{y'_j}{adv}$ plays the role of a source term. This can be solved by relaxation. Let $\delta\Gamma_j = \Gamma_j^{n+1} - \Gamma_j^n$ and ω be the relaxation factor. The iterative process reads:

$$\begin{aligned} \frac{\partial C_D}{\partial \Gamma_j} =& -8(a_{j-1,j} - a_{j,j})(y_j - y_{j-1})\frac{\delta\Gamma_j}{\omega} - 4\left(\frac{y'_j}{adv} + w_j\right)(y_j - y_{j-1}) \\ & - 4\sum_{k=2}^{jx-1}\Gamma_k(a_{j-1,k} - a_{j,k})(y_j - y_{j-1}) \qquad (12) \\ =& 0\ , \qquad j = 2, ..., jx-1 \qquad (13) \end{aligned}$$

With $jx = 101$ and $\omega = 1.8$ the solution converges in a few hundreds iterations. The solution obtained corresponds to a certain torque. In order to prescribe the torque, a constraint must be added. Define the cost functional to be $Cost = C_D + \lambda C_\tau$. λ is the Lagrange multiplier that will control the torque in the solution.

Taking derivatives of C_τ

$$\frac{\partial C_\tau}{\partial \Gamma_j} = 4(1+u_j)y'_j(y_j - y_{j-1}) + 4\sum_{k=2}^{jx-1}\Gamma_k(b_{j-1,k} - b_{j,k})y'_k(y_k - y_{k-1}) \ , \qquad j = 2,\ldots,jx-1 \tag{14}$$

In iterative form this reads

$$\frac{\partial C_\tau}{\partial \Gamma_j} = 8(b_{j-1,j} - b_{j,j})y'_j(y_j - y_{j-1})\frac{\partial \Gamma_j}{\omega} + 4(1+u_j)y'_j(y_j - y_{j-1}) \tag{15}$$

$$+ 4\sum_{k=2}^{jx-1}\Gamma_k(b_{j-1,k} - b_{j,k})y'_k(y_k - y_{k-1}) \ , \qquad j = 2,\ldots,jx-1 \tag{16}$$

Combining the above results, the change of circulation between two iterations is given by

$$2\left[a_{j,j} - a_{j-1,j} - \lambda(b_{j,j} - b_{j-1,j})y'_j\right](y_j - y_{j-1})\frac{\partial \Gamma_j}{\omega} = \left[\frac{y'_j}{adv} + w_j - \lambda(1+u_j)y'_j\right](y_j - y_{j-1})$$
$$+ \sum_{k=2}^{jx-1}\Gamma_k\left[a_{j-1,k} - a_{j,k} - \lambda(b_{j-1,k} - b_{j,k})y'_k\right](y_k - y_{k-1}) \ , \ j = 2,\ldots,jx-1 \tag{17}$$

In order to find the value of the Lagrange multiplier that will correspond to the desired value of the torque coefficient, say $C_{\tau target}$, let's note that C_D and C_τ can be decomposed into a linear and a bilinear forms in terms of the Γ_j's

$$C_D = C_{D1} + C_{D2} = -4\sum_{k=2}^{jx-1}\Gamma_k\frac{y'_k}{adv}(y_k - y_{k-1}) - 4\sum_{k=2}^{jx-1}\Gamma_k w_k(y_k - y_{k-1}) \tag{18}$$

$$C_\tau = C_{\tau 1} + C_{\tau 2} = 4\sum_{k=2}^{jx-1}\Gamma_k y'_k(y_k - y_{k-1}) + 4\sum_{k=2}^{jx-1}\Gamma_k u_k y'_k(y_k - y_{k-1}) \tag{19}$$

$$C_{D1} = -\frac{C_{\tau 1}}{adv} \tag{20}$$

C_{D1} and $C_{\tau 1}$ are homogeneous of degree one. C_{D2} and $C_{\tau 2}$ are homogeneous of degree two. Using the properties of homogeneous forms, the summation of the minimization equations multiplied each by the corresponding Γ_j results in the identity

$$\sum_{j=1}^{jx}\left(\frac{\partial C_D}{\partial \Gamma_j} + \lambda\frac{\partial C_\tau}{\partial \Gamma_j}\right)\Gamma_j = C_{D1} + 2C_{D2} + \lambda\left(C_{\tau 1} + 2C_{\tau 2}\right) = 0 \tag{21}$$

If we assume that the optimum distributions of circulation for different $C_{\tau target}$ vary approximately by a multiplication factor, then knowing the solution Γ_j for a particular value of λ (say $\lambda = 0$) allows to find a new value of the Lagrange multiplier as follows. Change the Γ_j's to new values $\kappa\Gamma_j$. In order to satisfy the constraint one must have $C_{\tau target} = \kappa C_{\tau 1} + \kappa^2 C_{\tau 2}$. Solving for κ yields

$$\kappa = \frac{\sqrt{C_{\tau 1}^2 + 4C_{\tau 2}C_{\tau target}} - C_{\tau 1}}{2C_{\tau 2}} \tag{22}$$

The new estimate for λ is obtained from the above identity as $\lambda = -\dfrac{C_{D1} + 2\kappa C_{D2}}{C_{\tau 1} + 2\kappa C_{\tau 2}}$. This procedure is repeated 2 or 3 times to produce the desired solution.

The optimum distributions of circulation and induced velocities for $adv = 0.1$, $P_\tau = 0.01$ and $y_0 = 0.1$ are shown in figures 2-4. Also shown is the effect of mesh refinement from $jx = 51$ to $jx = 101$. The fine mesh result is an accurate solution to the integro-differential equation.

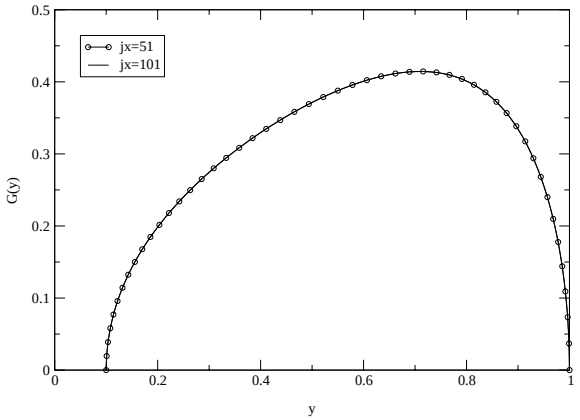

$(adv = .1,\ P_\tau = .01,\ y_0 = .1)$

Fig.2: Optimum distribution of circulation

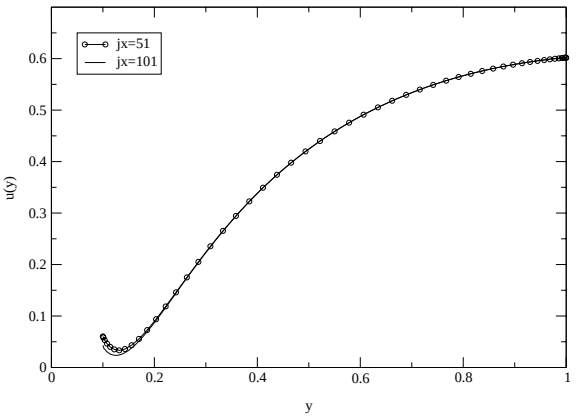

$(adv = .1,\ P_\tau = .01,\ y_0 = .1)$

Fig.3: Optimum distribution of axial velocity

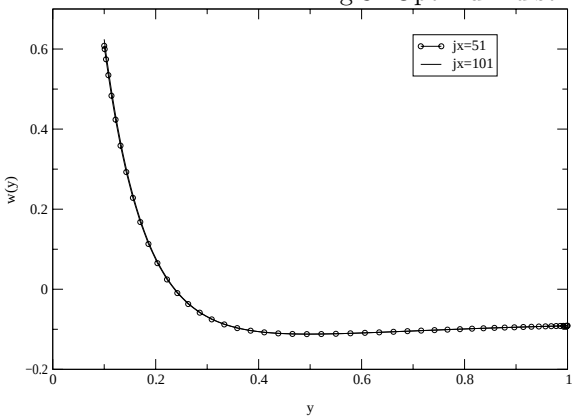

$(adv = .1,\ P_\tau = .01,\ y_0 = .1)$

Fig.4: Optimum distribution of downwash

4 Viscous correction

The viscous correction accounts for second order effects. It is assumed that the Reynolds number is large and that the boundary layer is attached. This is reasonable in a design procedure since the chord distribution can be chosen such that the lift coefficient remains well below the maximum lift coefficient in any section of the blade. Let $C_l(y)$ and $C_d(y)$ be the usual lift and drag coefficients of the two dimensional blade section.

The dimensional form of the elementary force on the blade section $(\ y, y+dy)$ is now

$$d\overrightarrow{F}(y) = \rho\,\overrightarrow{q}(y) \wedge \Gamma(y)\,\overrightarrow{j}\,dy + \frac{1}{2}\rho\,\|\,\overrightarrow{q}(y)\|\,\overrightarrow{q}(y) C_d(y) c(y) dy \tag{23}$$

where $\overrightarrow{q}$ is the local incoming flow velocity in the $(\ x, z)$-plane. Projection of the force on the x-axis and the z-axis yields the dimensionless force and moment coefficients for a two-bladed propeller

$$\begin{cases} C_D = -\,4\displaystyle\int_{y_0}^{1} \Gamma(y)\left(\frac{y}{adv} + w(y)\right) dy + 2\int_{y_0}^{1} \sqrt{(1+u(y))^2 + \left(\frac{y}{adv} + w(y)\right)^2}\,(1+u(y))\,C_d(y)c(y)dy \\ C_L = 4\displaystyle\int_{y_0}^{1} \Gamma(y)\,(1+u(y))\,dy + 2\int_{y_0}^{1} \sqrt{(1+u(y))^2 + \left(\frac{y}{adv} + w(y)\right)^2}\left(\frac{y}{adv} + w(y)\right) C_d(y)c(y)dy \\ C_\tau = 4\displaystyle\int_{y_0}^{1} \Gamma(y)\,(1+u(y))\,y dy + 2\int_{y_0}^{1} \sqrt{(1+u(y))^2 + \left(\frac{y}{adv} + w(y)\right)^2}\left(\frac{y}{adv} + w(y)\right) C_d(y)c(y)y dy \end{cases} \tag{24}$$

The propeller efficiency is $\eta = -\dfrac{VT}{\tau\Omega} = -adv\dfrac{C_D}{C_\tau}$.

Note that the chord distribution $c(y)$ is now explicitly in the formulation. It can be prescribed once for all or it can be part of the design process. At any rate, an initial chord distribution is needed. This system is nonlinear due to the viscous correction. To simplify the iteration process, only the dependency of C_d on Γ in the viscous terms will be used in the minimization process, all the other terms being frozen from the previous iteration. However, the above equations will be satisfied at convergence.

In order to obtain a minimization equation with a linear contribution in Γ from the viscous terms, we approximate the profile polar by piecewise parabolic curves as

$$\begin{aligned} C_d(C_l) =& C_{dm-1} + \frac{C_{dm} - C_{dm-1}}{C_{lm} - C_{lm-1}} (C_l - C_{lm-1}) \\ &+ \frac{(C_{dm+1} - C_{dm})(C_{lm} - C_{lm-1}) - (C_{dm} - C_{dm-1})(C_{lm+1} - C_{lm})}{(C_{lm+1} - C_{lm})(C_{lm+1} - C_{lm-1})(C_{lm} - C_{lm-1})} (C_l - C_{lm-1})(C_l - C_{lm}) \end{aligned} \quad (25)$$

were the indices ($m-1, m, m+1$) correspond to 3 consecutive points on the polar. The relation between the lift coefficient C_l and the circulation Γ is $C_l = \dfrac{2\Gamma}{\|\overrightarrow{q}\| c}$.

The formula for the local drag coefficient can be rewritten in compact form as $C_d = (C_{d0})_m + (C_{d1})_m C_l + (C_{d2})_m C_l^2$.

Let $C_{Di} = C_{D1} + C_{D2}$ and $C_{\tau i} = C_{\tau 1} + C_{\tau 2}$ (i for inviscid or induced) and the new cost functional be $Cost = C_{Di} + C_{Dv} + \lambda (C_{\tau i} + C_{\tau v})$, where the discrete analogs of the viscous terms are

$$\begin{cases} C_{Dv} = 2 \displaystyle\sum_{k=2}^{jx-1} q_k (1+u_k) \times \left((C_{d0})_{m(k)} + (C_{d1})_{m(k)} C_{lk} + (C_{d2})_{m(k)} C_{lk}^2 \right) c_k (y_k - y_{k-1}) \\ C_{\tau v} = 2 \displaystyle\sum_{k=2}^{jx-1} q_k \left(\frac{y'_k}{adv} + w_k \right) \times \left((C_{d0})_{m(k)} + (C_{d1})_{m(k)} C_{lk} + (C_{d2})_{m(k)} C_{lk}^2 \right) c_k y'_k (y_k - y_{k-1}) \end{cases} \quad (26)$$

and $q_k = \sqrt{(1+u_k)^2 + \left(\dfrac{y'_k}{adv} + w_k \right)^2}$ is the dimensionless incoming velocity.

In turn, we can decompose the viscous contributions into 3 terms, one independent of Γ, one linear and one quadratic function of Γ as $C_{Dv} = C_{Dv0} + C_{Dv1} + C_{Dv2}$ and $C_{\tau v} = C_{\tau v0} + C_{\tau v1} + C_{\tau v2}$. The partial derivatives in relaxation form read:

$$\begin{cases} \dfrac{\partial C_{Dv}}{\partial \Gamma_j} = 16 \dfrac{(1+u_j)(C_{d2})_{m(j)} (y_j - y_{j-1})}{q_j c_j} \dfrac{\delta \Gamma_j}{\omega} + 4(1+u_j) \left((C_{d1})_{m(j)} + 4 \dfrac{(C_{d2})_{m(j)} \Gamma_j}{q_j c_j} \right) (y_j - y_{j-1}) \\ \dfrac{\partial C_{\tau v}}{\partial \Gamma_j} = 16 \dfrac{\left(\dfrac{y'_j}{adv} + w_j \right) (C_{d2})_{m(j)} (y_j - y_{j-1})}{q_j c_j} \dfrac{\delta \Gamma_j}{\omega} + 4 \left(\dfrac{y'_j}{adv} + w_j \right) \left((C_{d1})_{m(j)} + 4 \dfrac{(C_{d2})_{m(j)} \Gamma_j}{q_j c_j} \right) (y_j - y_{j-1}) \end{cases} \quad (27)$$

The update of the Lagrange multiplier proceeds along similar lines as in the inviscid case. Now κ and λ are defined as

$$\kappa = \frac{\sqrt{(C_{\tau 1} + C_{\tau v1})^2 + 4(C_{\tau 2} + C_{\tau v2})(C_{\tau target} - C_{\tau 0})} - (C_{\tau 1} + C_{\tau v1})}{2(C_{\tau 2} + C_{\tau v2})} \quad (28)$$

$$\lambda = -\frac{C_{D1} + 2\kappa C_{D2} + C_{Dv1} + 2\kappa C_{Dv2}}{C_{\tau 1} + 2\kappa C_{\tau 2} + C_{\tau v1} + 2\kappa C_{\tau v2}} \quad (29)$$

In inviscid flow theory, the chord distribution as well as other geometrical characteristics do not appear in the optimization. Hence, there is an infinite number of blade geometries that will produce the optimum distribution

of Γ. A similar situation is known to exist for a profile or a large aspect ratio wing. On the other hand, the viscous problem is in all generality unmanageable. However, using a single known profile freezes the relative thickness and camber and reduces the problem to finding the optimum chord and twist distributions, given the profile polar at the appropriate Reynolds number. Again, the flow is assumed to be attached in design conditions. Some insight into the design can be gained by studying particular situations of interest, such as light loading for a wing or a propeller. Let's consider first a wing. As $adv \to \infty$, $u \to 0$, the cost functional reduces to

$$Cost = -4\int_{-1}^{1}\Gamma(y)w(y)dy + 2\int_{-1}^{1}C_d(y)c(y)dy + 4\lambda\int_{-1}^{1}\Gamma(y)dy \tag{30}$$

Since the viscous effects are only a small deviation of the inviscid solution, to first order the distribution of circulation is elliptic and the downwash w is constant. Taking the Frechet derivative, the minimization equation reads

$$\frac{\partial Cost}{\partial\Gamma}(\delta\Gamma) = -4\int_{-1}^{1}\delta\Gamma\left(w - \frac{dC_d}{dC_l} - \lambda\right)dy = 0 \tag{31}$$

This is satisfied when $\dfrac{dC_d}{dC_l}$ is constant along the span. At design conditions, away from maximum lift, the drag coefficient is a function of the lift, $C_d = C_d\left(C_l\right)$, hence the lift coefficient and the effective angle of attack are also constant along the wing. The value $\left(C_l\right)_{opt}$ for minimum drag corresponds to maximum $\dfrac{C_l}{C_d}$.

In the case of a propeller, assuming low advance ratio, the cost functional now reads

$$Cost = -4\int_{y_0}^{1}\Gamma(y)\frac{y}{adv}dy + 2\int_{y_0}^{1}q(y)C_d(y)c(y)dy + 4\lambda\int_{y_0}^{1}\Gamma(y)ydy \tag{32}$$

where $q(y) = \sqrt{1+\left(\dfrac{y}{adv}\right)^2}$

The minimization equation follows

$$\frac{\partial Cost}{\partial\Gamma}(\delta\Gamma) = -4\int_{y_0}^{1}\delta\Gamma\left(1 - \frac{dC_d}{dC_l} - \lambda adv\right)\frac{y}{adv}dy = 0 \tag{33}$$

Again, the minimum is obtained when the blade works at constant $\left(C_l\right)_{opt}$.

The design procedure consists in specifying an initial chord distribution, say constant chord c, large enough to produce a first solution with a lift coefficient below $\left(C_l\right)_{max}$. Then a new chord distribution is calculated as

$$c(y) = \frac{2\Gamma(y)}{\|\overrightarrow{q}(y)\|\left(C_l\right)_{opt}} \tag{34}$$

This is repeated until the chord distribution is converged. It was found that 5 design cycles were sufficient to obtain a converged solution.

5 Test case

The design of a propeller for $adv = 0.223$, $P_\tau = 0.01$ and $y_0 = 0.174$ is compared with that of Adkins and Liebeck [6]. The blade section is the NACA 4415 at Reynolds number 10^6. The polar characteristics are calculated using Drela's XFOIL code [9]. The angle of attack is swept from -3 degrees to 25 degrees by steps of 1 degree. It is found that $(C_l)_{opt} = 1.2$ for $\alpha = 6.8$ degrees. The data are shown in figure 5.

The distributions of Γ, u and w are shown in figure 6. The agreement is fair. It is clear that enforcing zero values for the induced velocities at the tip, as is done in reference [6], is not correct. Surprisingly the efficiencies compare well: $\eta_{A\&L} = 0.86996$, $\eta_{present\,method} = 0.8695$. This coincidence is fortuitous since the models are different and the Adkins and Liebeck calculation relies only on 6 radial control points.

The geometry of the blade is determined by the chord distribution and the twist. The leading and trailing edges locations versus y are shown in figure 7, where the quarter-chord has been placed along the y-axis. The setting or twist angle $t(y)$ measured from the x-axis is presented in figure 8.

Another important parameter is the flow angle measured from the z-axis given by $\tan(\phi(y)) = \dfrac{1+u(y)}{\dfrac{y}{adv}+w(y)} = \cot(t(y)+\alpha(y))$, where $\alpha(y)$ is the effective incidence. $\phi(y)$ is essentially driven by the advance ratio. It is compared with the results of reference [6] in figure 9.

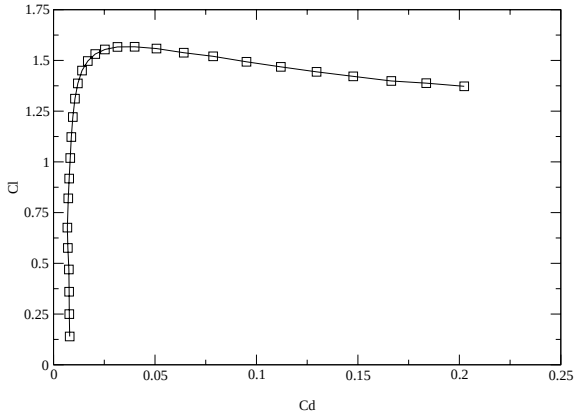

Fig.5: Calculated polar for the NACA 4415 at $R_e = 10^6$ (reference [9])

The propeller design obtained at $adv = 0.223$ is tested for a range of advance ratios, for the fixed power output $P_\tau = 0.01$ used in the design. The same governing equations are used. The results are presented in figure 10. At $adv = 0.18$, the maximum lift coefficient $(C_l)_{max} = 1.567$ is almost reached at the root section where $C_l = 1.563$. At $adv = 0.35$ the root section bears no lift. At $adv = 0.4$, half of the blade is functioning as a windmill with negative C_l.

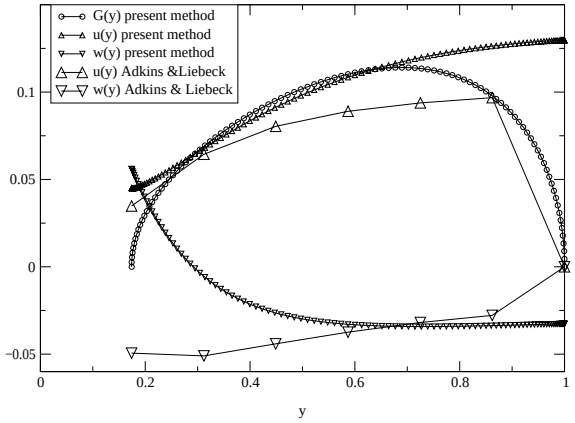

Fig.6: Comparison of the optimum design with results of reference [6]

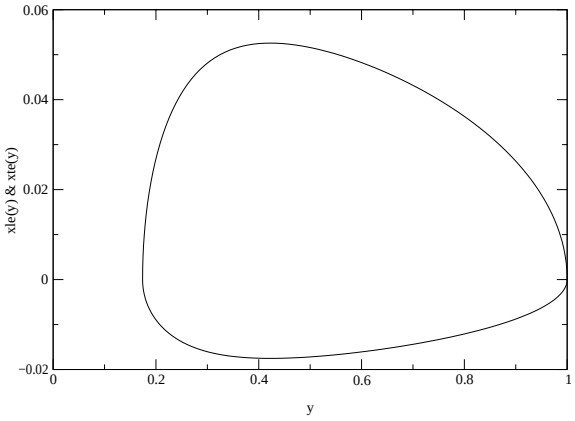

Fig.7: Chord distribution for the optimum design

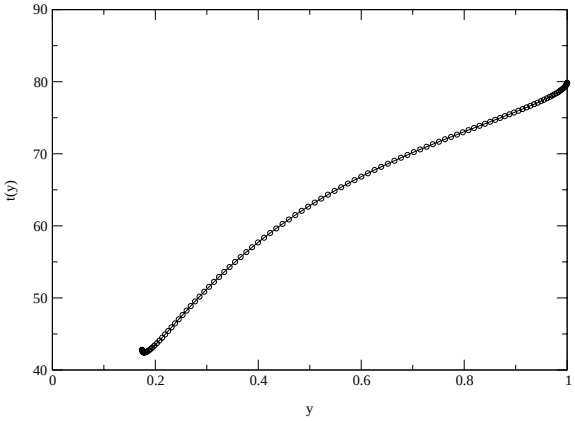

Fig.8: Distribution of twist along the blade

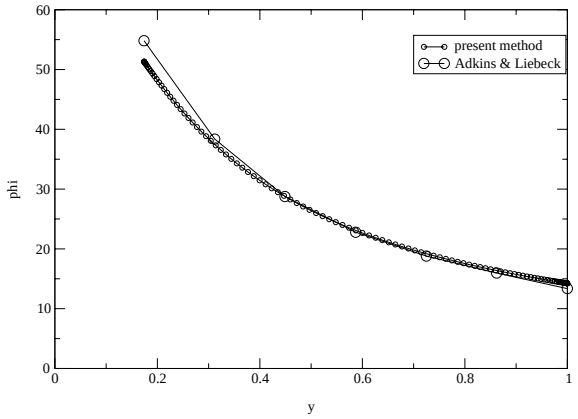

Fig.9: Comparison of flow angles

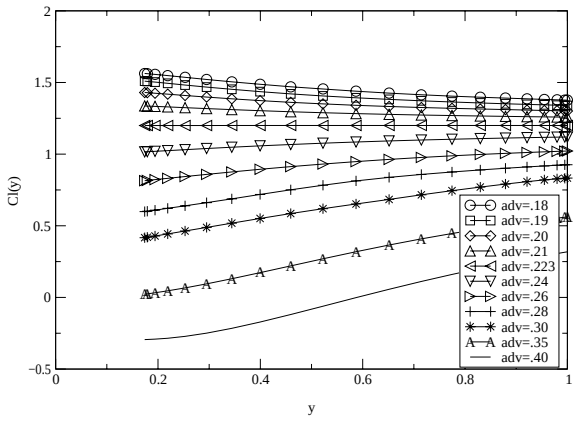

Fig.10: Lift coefficient distribution for a range of advance ratios

6 Conclusion

An improved model for the optimization of propellers, using the Goldstein model for the vortex structure and the Biot-Savart law for the flow interaction, has been established, based on the maximization of the thrust for a given torque. The inviscid model is corrected with two-dimensional viscous data from experiments or computation, using strip theory. However, interaction between the various blade sections is allowed with this model, in a way similar to the Prandtl lifting line theory. The results indicate that the method is flexible and efficient. The lifting line results are recovered accurately for large advance ratios. The design of a blade at low advance ratio compares well with previous results. The optimum geometry is also tested at off-design advance ratios, up to stall, using an analysis code based on the same formulation. This development allows to study the efficiency of the propeller in different working conditions and select the advance ratio that will produce the best overall design.

REFERENCES

[1] Prandtl, L. and Betz, A., "Vier Abhandlungen zur Hydrodynamik und Aerodynamik," Gottingen Nachr., Gottingen, Selbstverlag des Kaiser Wilhelm-instituts fur Stromungsforschung, 1927.

[2] Glauert, H., "Airplane Propellers," in Aerodynamic Theory, edited by W. F. Durand, Dover, Vol IV, 1963, pp. 169-269.

[3] Goldstein, S., "On the Vortex Theory of Screw Propellers," Proceedings of the Royal Society of London, Series A, Vol. 123, 1929, pp. 440-465.

[4] Lock, C., "Application of Goldstein's Airscrew Theory to Design," Aeronautical Research Committee, RM 1377, Nov. 1930.

[5] Theodorsen, T., Theory of Propellers, McGraw-Hill, 1948.

[6] Adkins, C. and Liebeck, R., "Design of Optimum Propellers," Journal of Propulsion and Power, Sept.-Oct. 1994, Vol 10, No 5, pp. 676-682.

[7] Wilson,R. and Lissaman, P., "Applied Aerodynamics of Wind Power Machines," Oregon State University, NSF-RA-N-74-113, PB 238 595, Corvallis, OR, May 1974.

[8] Chattot, J.-J., "Optimization in Applied Aerodynamics," Computational Fluid Dynamics Journal, Vol. 9, No. 3, Oct. 2000.

[9] Drela, M., and Giles, M.B., "Viscous-Inviscid Analysis of Transonic and Low Reynolds Number Airfoils," AIAA Journal, Vol. 25, No. 10, 1987, pp. 1347-1355.